American Mineralogist, Volume 101, pages 2095–2107, 2016

Carlsonite, $(NH_4)_5Fe^{3+}_3O(SO_4)_6\cdot 7H_2O$, and huizingite-(Al), $(NH_4)_9Al_3(SO_4)_8(OH)_2\cdot 4H_2O$, two new minerals from a natural fire in an oil-bearing shale near Milan, Ohio

Anthony R. Kampf[1,*], R. Peter Richards[2], Barbara P. Nash[3], James B. Murowchick[4], and John F. Rakovan[5]

[1]Mineral Sciences Department, Natural History Museum of Los Angeles County, 900 Exposition Boulevard, Los Angeles, California 90007, U.S.A.
[2]Geology Department, Oberlin College, Oberlin, Ohio 44074, U.S.A.
[3]Department of Geology and Geophysics, University of Utah, Salt Lake City, Utah 84112, U.S.A.
[4]Department of Geosciences, University of Missouri-Kansas City, 420 Flarsheim Hall, 5110 Rockhill Road, Kansas City, Missouri 64110, U.S.A.
[5]Department of Geology and Environmental Earth Science, Miami University, Oxford, Ohio 45056, U.S.A.

Abstract

The new minerals carlsonite (IMA2014-067), $(NH_4)_5Fe^{3+}_3O(SO_4)_6\cdot 7H_2O$, and huizingite-(Al) (IMA2015-014), $(NH_4)_9Al_3(SO_4)_8(OH)_2\cdot 4H_2O$, formed from a natural fire in an oil-bearing shale near Milan, Ohio. Carlsonite crystals are yellow to orange-brown thick tablets, flattened on {001}, or stout prisms, elongated on [110], up to about 0.5 mm in size. The mineral has a tan streak, vitreous luster, Mohs hardness of 2, brittle tenacity, irregular fracture, perfect {001} cleavage, calculated density of 2.167 g/cm^3, and is easily soluble in H_2O. Carlsonite is optically biaxial (–), α = 1.576(1), β = 1.585(1), and γ = 1.591(1) (white light). Huizingite-(Al) crystals, typically intergrown in light greenish yellow drusy aggregates, are tabular to bladed, flattened on {100}, up to about 0.25 mm in maximum dimension. The mineral has a white streak, vitreous luster, Mohs hardness of 2½, brittle tenacity, irregular fracture, no cleavage, calculated density of 2.026 g/cm^3, and is easily soluble in H_2O. Huizingite-(Al) is optically biaxial (+) with α = 1.543(1), β = 1.545(1), and γ = 1.563(1) (589.6 nm light). Raman and infrared spectroscopy was conducted on both minerals. Electron microprobe analyses provided the empirical formulas $[(NH_4)_{4.64}Na_{0.24}K_{0.12}]_{\Sigma 5.00}Fe^{3+}_{3.05}O(SO_4)_6\cdot 6.93H_2O$ and $[(NH_4)_{8.76}Na_{0.22}K_{0.02}]_{\Sigma 9.00}(Al_{1.65}Fe^{3+}_{1.34})_{\Sigma 2.99}(OH)_{1.98}(H_2O)_{4.02}(SO_4)_{8.00}$ for carlsonite and huizingite-(Al), respectively. Huizingite compositions with Fe > Al were noted. Carlsonite is triclinic, $P\bar{1}$, a = 9.5927(2), b = 9.7679(3), c = 18.3995(13) Å, α = 93.250(7)°, β = 95.258(7)°, γ = 117.993(8)°, V = 1506.15(16) Å^3, and Z = 2. Huizingite-(Al) is triclinic, $P\bar{1}$, a = 9.7093(3), b = 10.4341(3), c = 10.7027(8) Å, α = 77.231(5)°, β = 74.860(5)°, γ = 66.104(5)°, V = 948.73(9) Å^3, and Z = 1. The five strongest lines in the X-ray powder diffraction pattern of carlsonite are [d_{obs} in Å(I)(hkl)]: 9.23(100)(002); 8.26(40)(100,011); 7.57(43)($\bar{1}$11,1$\bar{1}$1,011); 4.93(23)($\bar{1}\,\bar{1}$1,$\bar{1}$20); and 3.144(41)(multiple). Those for huizingite-(Al) are: 8.82(60)(100); 5.04(69)(121); 3.427(100)($\bar{2}\,\bar{2}$1); 3.204(68)($\bar{2}$11); and 3.043(94)(2$\bar{1}$2,312).

The crystal structures of carlsonite (R_1 = 0.030) and huizingite (R_1 = 0.040) are bipartite, each consisting of a structural unit and an interstitial unit. For carlsonite, the structural unit is a $[Fe^{3+}_3O(H_2O)_3(SO_4)_6]^{5-}$ cluster and the interstitial complex is $[(NH_4)_5(H_2O)_4]^{5+}$. For huizingite-(Al), the structural unit is a $[(Al,Fe^{3+})_3(OH)_2(H_2O)_4(SO_4)_6]^{5-}$ cluster and the interstitial complex is $[(NH_4)_9(SO_4)_2]^{5+}$. In the carlsonite cluster, three FeO_6 octahedra share a common vertex, while in the huizingite-(Al) cluster, three $(Al,Fe)O_6$ octahedra form an abbreviated corner-linked chain. The cluster in carlsonite is the same as that in metavoltine, while the huizingite-(Al) cluster is unique. The range of Lewis basicity of the structural unit in carlsonite is 0.23–0.11 valence units (v.u.) and in huizingite-(Al) it is 0.20–0.12 v.u.; the corresponding Lewis acidities of the interstitial complexes in these structures are 0.13 and 0.14 v.u., respectively. A characteristic Lewis acid strength of 0.13 v.u. is suggested for NH_4^+ when it is in its most typical coordinations of 7 to 8. The close structural relationship between carlsonite and metavoltine and the similarity of their powder diffraction patterns suggests that carlsonite may have misidentified as metavoltine in some NH_4-rich mineral assemblages. The new heteropolyhedral cluster in the structure of huizingite-(Al) is of interest because its existence may provide insights into the structural and paragenetic relations among hydrated ferric sulfate minerals. In particular, it may exist as a complex in aqueous solutions or in solid-state transformations involving the formation and/or breakdown of sideronatrite-style $[Fe^{3+}(SO_4)_3]^{3-}$ chains. We surmise that it may be a more commonly formed mineral than its abundance would indicate and that its rarity may reflect a narrow stability range, and so a transitory existence.

Keywords: Carlsonite, huizingite-(Al), new mineral, crystal structure, Raman spectroscopy, infrared spectroscopy, Lewis acidity-basicity, Huron Shale burn site, Milan, Ohio

Introduction

This paper reports the descriptions of the first two terrestrial (non-meteoritic) minerals to have been first discovered in the state of Ohio. These minerals, carlsonite and huizingite-(Al), formed as the result of a non-anthropogenic fire in an oil-bearing shale along the Huron River.

Carlsonite is named for Ernest H. Carlson (1933–2010). Carlson (Ph.D., McGill University 1966) was professor of mineralogy at Kent State University in Kent, Ohio, from 1966 until his retirement in 2009. He was a Fellow of both the Society

* E-mail: akampf@nhm.org

of Economic Geologists and the Association of Exploration Geochemists. Carlson is perhaps best known for his studies of Ohio minerals and his authorship of Ohio Geological Survey Bulletin 69, *Minerals of Ohio* (1991). At the time of his death, Carlson was engaged in initial studies of the minerals of the Huron Shale burn site at which carlsonite and huizingite-(Al) were found, and he performed some of the early identifications of the minerals from this occurrence.

Huizingite is named for Terry E. Huizing (born 1938) and Marie E. Huizing (born 1939) of Cincinnati, Ohio. Terry has been an avid mineral collector since childhood. He and Marie met in college and married in 1961 following graduation, he with a B.S. in chemical engineering and she with a degree in secondary education with a major in English. Marie caught the mineral-collecting bug from Terry and both became (and still are) very active in the Cincinnati Mineral Society. Marie wrote and edited the society's newsletter, *The Quarry*, for more than 15 years. She was asked to assume the duties of Editor of *Rocks & Minerals* in 1978, a job that she has very effectively executed ever since, with Terry at her side serving as a Consulting Editor and helping with the promotion of the magazine. Terry has also served as North American representative for several other mineralogical publications, has published several mineralogical articles and, since the late 1970s, has served as the Adjunct Curator of Mineralogy for the Cincinnati Museum Center (formerly the Cincinnati Museum of Natural History). In recognition of these and many other contributions to the Earth sciences, both Terry and Marie have received numerous honors. Terry received the Cincinnati Mineral Society Educational Foundation Award in 1984 and the American Federation Scholarship Foundation Award in 1991 for "distinguished achievement in the field of earth sciences." Marie received the Cincinnati Mineral Society Educational Foundation Award in 1978, the Carnegie Mineralogical Award for 1995, and the Mineralogical Society of America's Distinguished Public Service Award for 2007. Terry and Marie Huizing have agreed to the naming of this mineral in their honor. The -(Al) suffix is used to indicate that this mineral is the Al-dominant member of a series with its not-yet-described Fe-dominant counterpart, for which the name huizingite-(Fe) is proposed.

The new minerals and their names were approved by the Commission on New Minerals, Nomenclature and Classification of the International Mineralogical Association [carlsonite: IMA2014-067; huizingite-(Al): IMA2015-014]. The carlsonite description is based on one holotype and one cotype specimen, both of which are deposited in the collections of the Natural History Museum of Los Angeles County, catalog numbers 65544 and 65545. The description of huizingite-(Al) is based on one holotype specimen, which is deposited in the collection of the Natural History Museum of Los Angeles County, catalog number 65576.

Occurrence

Carlsonite and huizingite-(Al) occur in a suite of minerals that resulted from a natural fire in an oil-bearing shale at the interface between an eroded stream cliff (up to 7.5 m high) and its talus pile (~4.5 m thick) along the Huron River in north-central Ohio, approximately 6.1 km WSW of Milan, Ohio, U.S.A. (41°16′41.4″N, 82°40′27.0″W). The fire started in September of 2009, as the result of spontaneous combustion, and burned until March of 2011 (Fig. 1). The occurrence is referred to as the Huron Shale burn site.

The rock unit exposed is the late Devonian Huron Shale member of the Ohio Shale Formation, a dark gray to black marine, carbon-rich shale containing ironstone concretions, finely divided pyrite and pyrite nodules, and >10% organic matter. A sample taken from a 4-m cliff exposure near Milan, about 6 km to the northeast of the fire site, yielded 5.2 gallons of oil per ton of shale (Hoover 1960). The geometry of the talus slope favors access of oxygen to pyrite, but also the sequestration of heat, which led to the spontaneous combustion. The fire was concentrated at the interface between talus slope and cliff, but burned away from the cliff into the talus pile in some areas. It burned to a depth of about 2 m. The mineral suite formed by deposition on the surfaces of rocks within the talus pile as gases from the fire cooled (Fig. 2). Surface temperatures at the vent were between 204 and 260 °C. A temperature probe operated by the Huron County Engineers Office registered a 426 °C reading at a depth of 0.5 m. These temperatures were measured during a moderately intense stage of the fire. The cliff and talus slope formed as the result of natural erosion; the fire occurred without any form of human intervention and was sustained naturally by the oil in the shale.

Minerals directly associated with carlsonite include anhydrite, boussingaultite, gypsum, and lonecreekite. Minerals

Figure 1. Huron Shale burn site along the Huron River near Milan, Ohio, in early 2011.

directly associated with huizingite-(Al) include adranosite-(Al), anhydrite, boussingaultite, mascagnite, and salammoniac. Other minerals in the assemblage include adranosite-(Fe), alunogen, boussingaultite, clairite, ferrinatrite, gypsum, halotrichite, kremersite, lonecreekite, mascagnite, metavoltine, pyracmonite, sabieite (2*H* and 3*R* polytypes; Kampf et al. 2014), salammoniac, sulfur, tschermigite, and voltaite.

Carlsonite and huizingite-(Al) are exceedingly rare minerals, thus far known only from a few specimens at a single occurrence, and neither has previously been reported as a synthetic phase. They formed at ambient pressure, but in an extreme and ephemeral environment characterized by a steep temperature gradient, indicating that they probably have very narrow stability ranges.

Appearance and properties

Carlsonite

Carlsonite crystals are thick tablets, flattened on {001}, or stout prisms, elongated on [110], up to about 0.5 mm in size (Fig. 3). The crystal forms observed are {100}, {001}, {1$\bar{1}$0}, {111}, (1$\bar{1}$ $\bar{1}$} and {01$\bar{2}$} (Fig. 4). Cross-hatched twinning was rarely observed under crossed polars. Carlsonite is yellow to orange-brown, with a tan streak. Crystals are transparent with vitreous luster and display no fluorescence. The Mohs hardness based upon scratch tests is 2. Tenacity is brittle, fracture is irregular, and cleavage is perfect on {001}. The density calculated based on the empirical formula using single-crystal unit-cell data is 2.167 g/cm^3. Crystals are easily soluble in room-temperature H_2O. The mineral is optically biaxial (–) with indices of refraction α = 1.576(1), β = 1.585(1), and γ = 1.591(1) determined in white light. The 2*V* measured directly using a spindle stage is 80(1)°. The calculated 2*V* is 78°. Strong *r* > *v* dispersion was observed. The incompletely determined optical orientation is $X \approx \perp\{001\}$, $Z \approx [110]$. The pleochroism is *X* yellow, *Y* and *Z* orange; $X < Y \approx Z$. The Gladstone-Dale compatibility index $1 - (K_p/K_c)$ is 0.001 for the empirical formula, in the range of superior compatibility (Mandarino 2007).

Figure 2. Recently formed minerals near the interface between the cliff face and talus slope. The white dendritic crystals are salammoniac. (FOV = 22 cm).

Huizingite-(Al)

Huizingite-(Al) crystals are tabular, on {100}, to bladed, up to about 0.25 mm in maximum dimension. Crystals are typically intergrown in drusy aggregates (Figs. 5 and 6). The crystal forms observed are {100}, {010}, {001}, and {110} (Fig. 7). No twinning was observed. Huizingite-(Al) is light greenish yellow, with a white streak. Crystals are transparent with vitreous luster and display no fluorescence. The Mohs hardness based upon scratch tests is 2½. Tenacity is brittle, fracture is irregular, and the mineral displays no cleavage. The density calculated based on the empirical formula using single-crystal cell data is 2.026 g/cm^3. Crystals are easily soluble in room-temperature H_2O. The mineral is optically biaxial (+) with indices of refraction α = 1.543(1), β = 1.545(1), γ = 1.563(1) determined using 589.6 nm light. The 2*V* measured directly using a spindle stage is 40(3)°. The calculated 2*V* is 37°. Strong *r* > *v* dispersion was observed. The optical orientation is *X* ^ **a** = 24°, *Y* ^ **b** = 25°, *Z* ^ **c** = 27°. The pleochroism is *X* pale yellow, *Y* and *Z* nearly colorless; $X > Y \approx Z$. Crystals exhibit irregularly zoned extinction, apparently related to Al:Fe compositional zonation. During conoscopic observation, the isogyres were quite diffuse, presumably due to the combination of zoned optical properties

Figure 3. Carlsonite crystal. (FOV = 1 mm).

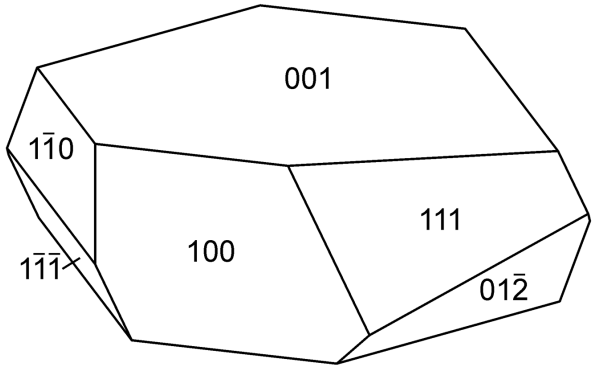

Figure 4. Crystal drawing of carlsonite tablet; clinographic projection in standard orientation.

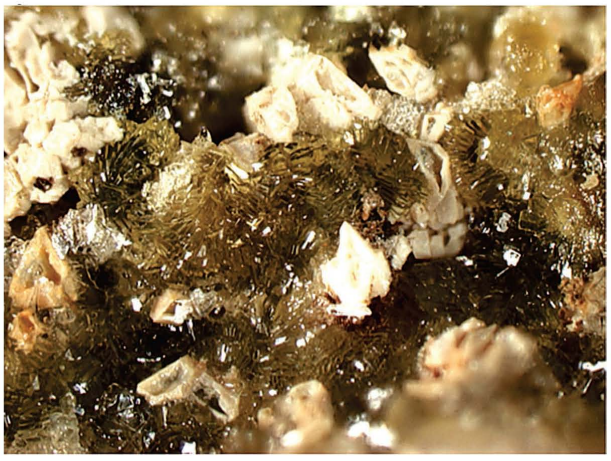

FIGURE 5. Drusy intergrowths of huizingite-(Al) crystals with anhydrite. (FOV = 2.2 mm across).

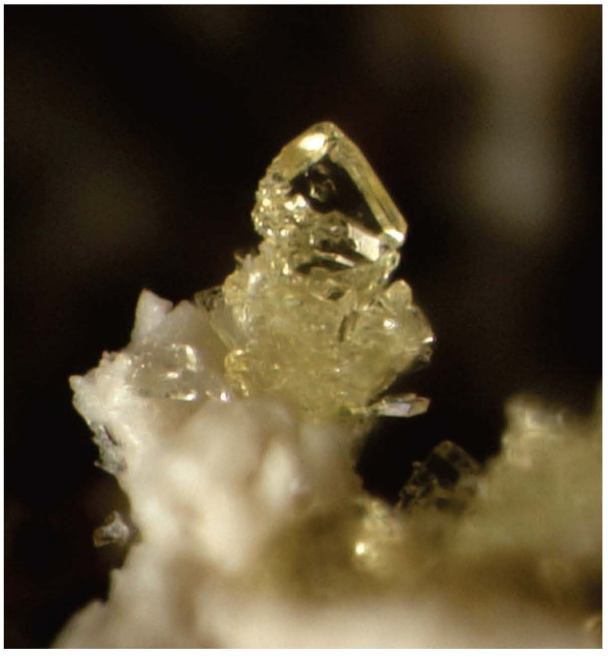

FIGURE 6. Huizingite-(Al) crystals on anhydrite. (FOV = 0.6 mm across).

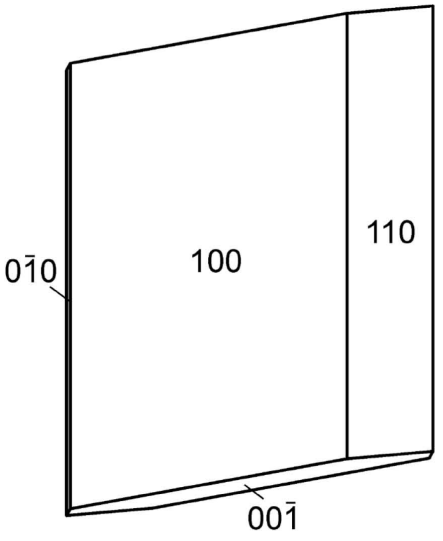

FIGURE 7. Crystal drawing of huizingite-(Al) tablet; clinographic projection in standard orientation.

and strong dispersion. The Gladstone-Dale compatibility index $1 - (K_P/K_C)$ is –0.015 for the empirical formula, in the range of superior compatibility (Mandarino 2007).

Raman and infrared spectroscopy

Raman analysis of single crystals of huizingite-(Al), within a 0.28 mm cluster of crystals, and a single crystal of carlsonite in a similar sized cluster were conducted with a Renishaw InVia Raman Microscope. The spectrometer interfaced to the microscope employed a 1800 groove/mm grating and a charge-coupled detector. The samples were excited using a HeNe laser (632 nm) that was focused onto the sample using a 20× (0.40 N.A.) objective for the huizingite and a 50× (0.85 N.A.) objective for carlsonite. The same objectives were employed to collect the backscattered Raman radiation. The spectra were collected with a spectral resolution of 4 cm^{-1}, over the range of 100–4000 cm^{-1}, using an integration time of 120 s per scan, and samples in unknown orientations. The collected spectra were essentially featureless above 1600 cm^{-1}. Five individual scans were averaged to produce the final Raman spectrum (Figs. 8 and 9). Abscissa values were calibrated using the phonon band of single-crystal silicon located at 520.7 ± 0.3 wavenumber.

The huizingite spectrum was collected at full laser power (10.0 mW) with no harm to the sample. The following intense bands are observed at (centroid positions in cm^{-1}): 223, 263, 448, 468, 478, 618, 641, 673, 980, 1003, 1010, 1027, 1064, 1123, 1151, and 1205. Most of the observed bands in the Raman spectra relate to the four structurally distinct SO_4^{2-} groups. Based on comparison to other sulfate minerals the following (speculative) band assignments can be made: (1) the most intense bands 980, 1003, 1010, and 1027 cm^{-1} are from the symmetric stretch, ν_1, of the four sulfate groups; (2) bands 1064, 1123, 1151, and 1205 cm^{-1} are from the ν_3 modes of the sulfate groups; (3) bands in the 618–673 cm^{-1} region are from the ν_4 modes of the sulfate groups; (4) bands in the 448–478 cm^{-1} region are from the ν_2 modes of the sulfate groups; and (5) bands at 223 and 263 cm^{-1} are uncertain but possibly due to $^{[VI]}$Fe-O modes.

The carlsonite spectrum was collected at 10% laser power (1.0 mW) because the full 10 mW beam caused sample burning and the formation of hematite, for which a sharp Raman spectrum was produced. After data collection, a 5 mW beam was used for further analysis and did not affect the sample. The following intense bands are observed at (centroid positions in cm^{-1}): 245, 275, 436, 487, 514, 552, 576, 617, 629, 670, 1015, 1066, 1104, 1140, 1160, 1188, and 1219. Band assignments are similar to those of huizingite-(Al).

Raman signals from structural ammonium and water, in the vicinity of 3300 cm^{-1}, were also investigated in both samples.

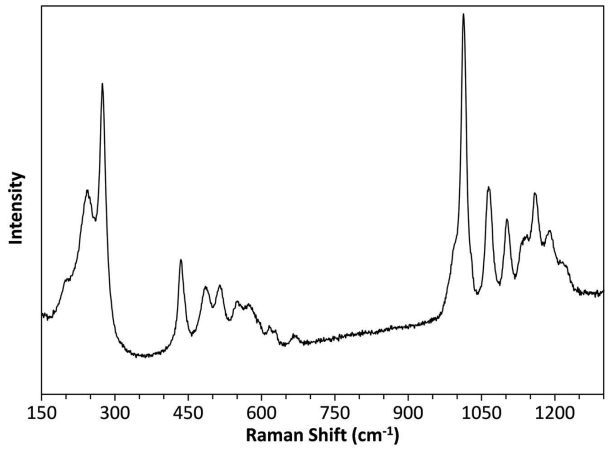

FIGURE 8. Raman spectrum of carlsonite.

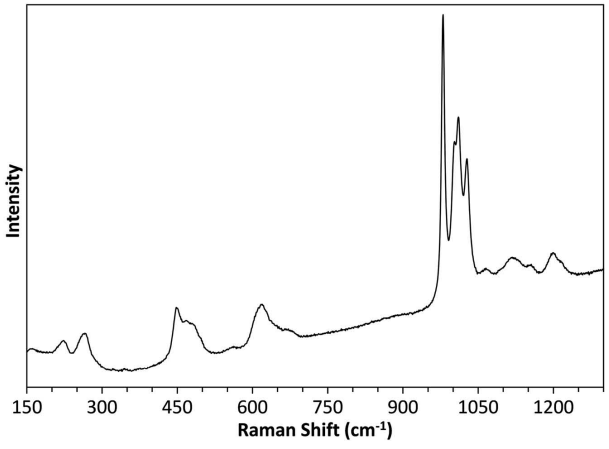

FIGURE 9. Raman spectrum of huizingite-(Al).

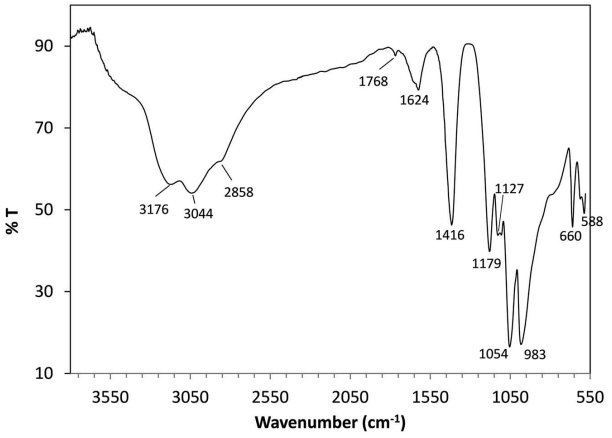

FIGURE 10. FTIR spectrum of carlsonite.

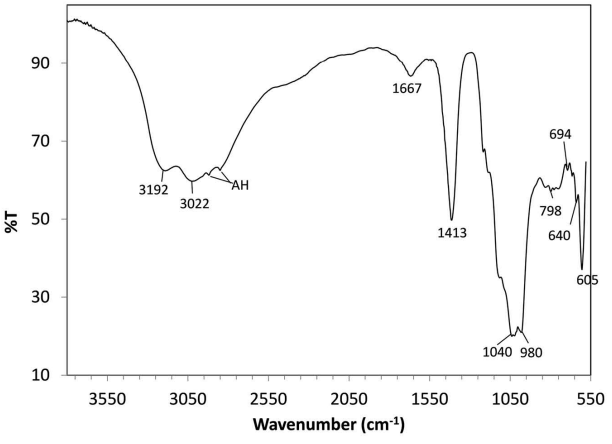

FIGURE 11. FTIR spectrum of huizingite-(Al).

For huizingite, there were no observable peaks in this region. With the 10.0 mW beam, a very weak but discernible envelope of peaks was observed around 3300 cm^{-1} in carlsonite; however, at lower powers these peaks were not detectable.

Although the presence of ammonium in huizingite was not detected in Raman and only a weak broad signal was observed in carlsonite, FTIR clearly shows the presence of ammonia in these two minerals. Attenuated total internal reflection (ATR) spectra were collected with a Perkin-Elmer Spotlight 400 infrared microscope interfaced to a Perkin-Elmer Spectrum One Fourier transform infrared spectrometer (FTIR). The system employed a 100 × 100 μm, liquid nitrogen cooled, mercury cadmium telluride (HgCdTe) detector. The standard drop-down germanium internal reflection element was employed in conjunction with a 50 × 50 μm aperture. Each spectrum collected (Figs. 10 and 11) represents the average of 128 individual scans possessing a spectral resolution of 4 cm^{-1}.

The normal vibrational modes of unbound ammonium have frequencies of 3033 = $\nu_1(A_1)$, 1680 = $\nu_2(E)$, 3137 = $\nu_3(F_2)$, and 1400 = $\nu_4(F_2)$ cm^{-1} (Nakamoto 1986). Of these only ν_3 and ν_4 are IR active; however, the lower symmetry sites of a crystal structure may allow the ν_1 and ν_2 modes to become active. The frequencies of these modes are also shifted as a result of bonding effects in carlsonite and huizingite. FTIR spectra clearly show the presence of ammonium in these minerals by the 1416 and 1413 cm^{-1} bands, respectively. Other modes are observable but their IR absorptions can be difficult to distinguish from those of structural water. For example, the 3044 and 3022 cm^{-1} bands, in these minerals, respectively, are likely the ν_1 mode in ammonium. The ammonium ν_3 mode appears at 3176 cm^{-1} in carlsonite and at 3192 cm^{-1} in huizingite. The band at 1667 cm^{-1} in huizingite is likely from the ammonium ν_2 vibrational mode, but a band in this region for carlsonite is not observed. In carlsonite the weak band with a maximum at 1624 is most likely the bending mode of the water molecules. This feature is not observed in the huizingite, possibly due to the lower water concentration and broadening of the signal due to hydrogen bonding. Finally, the broad shoulder around 3500 cm^{-1} in carlsonite is likely from the OH stretching modes in water that may, in part, also contribute to the band associated with ammonium in the vicinity of 3300 cm^{-1} (Szakall et al. 2012). Thus, there is an absence of or weak contribution by typical H_2O absorptions, especially in the OH stretching region. Similar results

were reported by Knop et al. (1985) for $(NH_4)_2[AlF_5(H_2O)]$. They concluded that the OH stretching absorption in that phase underlies the group of peaks in the 3100–2900 cm^{-1} region that result from ammonium absorptions.

Chemical composition

Analyses of carlsonite (7 on six crystals) and huizingite-(Al) (10 on four crystals) were performed at the University of Utah on a Cameca SX-50 electron microprobe with four wavelength-dispersive spectrometers utilizing Probe for EPMA software (Probe Software, Inc.). A 15 keV accelerating voltage and a 20 μm beam diameter were used for both minerals; a 20 nA beam current was used for carlsonite and a 10 nA beam current was used for huizingite-(Al). Counting times were 40 s for N and 20 s for other elements. Nitrogen was analyzed with a 60 Å W/Si multilayer pseudocrystal (Cameca PC-1). The sample and nitrogen standard (synthetic AlN) were carbon-coated at the same time to assure an equivalent thickness of the carbon layer. Other standards employed are albite (Na), sanidine (K), hematite (Fe), and celestine (S). Raw X-ray intensities were corrected for matrix effects with a $\phi(\rho z)$ (PAP) algorithm (Pouchou and Pichoir 1991).

Electron microprobe analysis of low atomic number elements such as nitrogen is complicated by a low cross section for ionization and high absorption of the soft X-rays. Our analyses confirmed the presence of significant N; however, our $(NH_4)_2O$ values are less than those predicted by the structures [50% of predicted for carlsonite and 86% of predicted for huizingite-(Al)]. The nature of the structure suggests that NH_4^+ is weakly bonded and some is probably quickly lost, along with H_2O, under vacuum, either initially during carbon coating of the sample or subsequently in the microprobe chamber. Monitoring of the N*K*α intensity during each spot analysis showed only a slight decrease in N concentration with time under the electron beam for which a correction was applied, but as noted above, it is likely that NH_3 was lost under vacuum prior to the analyses. Unfortunately, there is insufficient material for direct determinations of N or H by CHN analysis. Consequently, the $(NH_4)_2O$ and H_2O contents were calculated by stoichiometry based upon the crystal-structure determinations. For carlsonite the high EPMA total after addition of calculated $(NH_4)_2O$ and H_2O is attributed to the loss of these constituents under vacuum, which results in higher concentrations for the remaining constituents. While the loss of $(NH_4)_2O$ and H_2O under vacuum should be expected to provide a high EPMA total for huizingite as well, in fact the analytical total was low. We attribute this to huizingite being very susceptible to beam damage, even when using low beam current and a 20 μm diameter defocused beam. The results for carlsonite are presented in Table 1a and those for huizingite in Table 1b.

The empirical formula for carlsonite (based on 6 S apfu) is $[(NH_4)_{4.64}Na_{0.24}K_{0.12}]_{\Sigma 5.00}Fe^{3+}_{3.05}O(SO_4)_6 \cdot 6.93H_2O$. The simplified formula is $(NH_4)_5Fe^{3+}_3O(SO_4)_6 \cdot 7H_2O$, which requires $(NH_4)_2O$ 13.34, Fe_2O_3 24.54, SO_3 49.21, H_2O 12.92, total 100%. The empirical formula for huizingite-(Al) (based on 38 O apfu) is $[(NH_4)_{8.76}Na_{0.22}K_{0.02}]_{\Sigma 9.00}(Al_{1.65}Fe^{3+}_{1.34})_{\Sigma 2.99}(SO_4)_{8.00}(OH)_{1.98} \cdot 4.02H_2O$. The simplified end-member formula is $(NH_4)_9Al_3(SO_4)_8(OH)_2 \cdot 4H_2O$, which for the Al end-member requires $(NH_4)_2O$ 20.96, Al_2O_3 13.68, SO_3 57.30, H_2O 8.06, total 100 wt%, and for the intermediate member with Al:Fe = 1 requires $(NH_4)_2O$ 20.18, Al_2O_3 6.59, Fe_2O_3 10.31, SO_3 55.16, H_2O 7.76, total 100 wt%.

Table 1a. Electron microprobe analytical results for carlsonite

Constant	wt%	Range	S.D.	Normalized
$(NH_4)_2O$	6.30	6.03–6.48	0.15	
$(NH_4)_2O$[a]	12.75			12.30
Na_2O	0.79	0.42–1.13	0.24	0.76
K_2O	0.59	0.47–0.72	0.09	0.57
Fe_2O_3	25.70	25.17–26.42	0.51	24.79
SO_3	50.67	49.87–51.73	0.79	48.88
H_2O[a]	13.16			12.70
Total	103.66			100.00

Table 1b. Electron microprobe analytical results for huizingite-(Al)

Constant	wt%	Range	S.D.	Normalized
$(NH_4)_2O$	15.88	14.71–17.27	0.85	
$(NH_4)_2O$[a]	18.57			19.70
Na_2O	0.55	0.30–1.05	0.27	0.58
K_2O	0.09	0.06–0.12	0.02	0.10
Al_2O_3	6.85	5.53–8.59	1.20	7.27
Fe_2O_3	8.71	6.40–10.17	1.36	9.24
SO_3	52.14	49.91–53.66	1.11	55.32
H_2O[a]	7.35			7.80
Total	94.26			100.00

[a] Based upon the crystal structure determination.

Among the 10 analyses of huizingite on which the results in Table 1b are based, the Al:Fe ratio ranged from 0.86 to 2.03 or, in terms of the empirical formula, from $(Al_{1.39}Fe_{1.61})$ to $(Al_{2.03}Fe_{0.99})$. Both Al- and Fe-dominant regions were found in every crystal analyzed and no spatial core-to-rim variation was found in a survey of Al and Fe contents over these and additional crystals. Our findings indicate that, on average, the crystals are significantly higher in Al than Fe and, in crystal regions where Fe is greater than Al, it is only slightly so. Of the 10 analyses included in Table 1, five are Al dominant (Al:Fe = 1.43–2.03) and five are Fe dominant (Al:Fe = 0.86–0.97). Furthermore, Al significantly dominates over Fe (on average) in the crystal used for the structure refinement $(Al_{1.72}Fe_{1.28})$. Because available material does not allow the characterization of the Fe-dominant phase and the material characterized here is, on average, Al dominant, we are describing only the Al-dominant phase. However, because we have demonstrated the existence of the Fe-dominant phase, we recommend the use of a suffix-based nomenclature for the end-members (Al- and Fe-dominant) of this series, i.e., huizingite-(Al) and huizingite-(Fe).

X-ray crystallography and structure determination

Both powder and single-crystal X-ray diffraction studies were carried out using a Rigaku R-Axis Rapid II curved imaging plate microdiffractometer, with monochromatized Mo*K*α radiation. For the powder-diffraction studies, a Gandolfi-like motion on the φ and ω axes was used to randomize the sample. Observed *d* values and intensities were derived by profile fitting using JADE 2010 software (Materials Data, Inc.). Data (in angstroms for Mo*K*α) are given in Table 2[1] along with the

[1]Deposit item AM-16-95680, Table 2 and CIF. Deposit items are free to all readers and found on the MSA web site, via the specific issue's Table of Contents (go to http://www.minsocam.org/MSA/AmMin/TOC/).

calculated pattern.

The Rigaku CrystalClear software package was used for processing intensity data, including the application of empirical multi-scan absorption corrections using ABSCOR (Higashi 2001). The structures were solved by direct methods using SIR2004 (Burla et al. 2005). SHELXL-2013 (Sheldrick 2008) was used for the refinements of the structures. For both structures, the location of all non-hydrogen sites was straightforward. After refinement of these sites with anisotropic displacement parameters, difference-Fourier maps provided the locations of all H atom sites associated with the H_2O and NH_4 groups in carlsonite and the OH, H_2O, and NH_4 groups in huizingite-(Al); however, the H sites associated with N5 in huizingite-(Al) are disordered and partially occupied, as can be expected for a NH_4 group on a center of symmetry (0,½,0). The H sites were refined using soft distance restraints with N–H = 0.90(3), O–H = 0.82(3), H–H of NH_4 = 1.45(3) and H–H of H_2O = 1.30(3) Å. The H–H restraint was not used for the disordered NH_4 group mentioned above. U_{eq} of each H was set to 1.2 times that of the N or O atom to which it is bonded. The refinement of the huizingite structure converged well with these restraints; however, the carlsonite refinement exhibited relatively large shifts in the final refinement cycle: maximum shift/s.u. = 1.323 and mean shift/s.u. = 0.036. The removal of the distance restraints allowed the refinement to converge nicely (maximum shift/su = 0.002 and mean shift/su = 0.000); however, some of the resulting N–H and O–H distances were significantly too high or too low. Consequently, we have elected to report the refinement of the carlsonite structure using the aforementioned restraints. Details of the sample, data collection, and structure refinement for each mineral are provided in Table 3, final atom coordinates and equivalent isotropic displacement parameters in Table 4, selected bond distances in Table 5, N-H-O bond distances and angles in Table 6, and bond-valence analyses in Table 7. Note that anisotropic displacement parameters are available in the deposited CIF[1].

Discussion of the structures

Carlsonite

Carlsonite is a bipartite structure that consists of a structural unit and an interstitial complex, as elucidated by Schindler and Hawthorne (2001). The $[Fe^{3+}_3O(H_2O)_3(SO_4)_6]^{5-}$ cluster defines the structural unit. The interstitial complex, ideally $[(NH_4)_5(H_2O)_4]^{5+}$, balances the charge of the structural unit and links the structural units together. The atomic arrangement of carlsonite is depicted in Figure 12 and the structural unit is shown in Figure 13.

A polytypic relationship may exist between carlsonite and clairite, $(NH_4)_2Fe_3(SO_4)_4(OH)_3\cdot 3H_2O$; however, clairite crystals are generally of too poor quality for definitive single-crystal study. Note that clairite is reported to be slowly soluble in H_2O (Martini 1983). Our examination of clairite crystals from the Huron Shale burn site confirmed them to be very slowly soluble, requiring several hours to dissolve. By contrast, carlsonite crystals are easily soluble in H_2O, arguing against a simple polytypic relationship between the species.

The $[Fe^{3+}_3O(H_2O)_3(SO_4)_6]^{5-}$ cluster in the structure of carlsonite (Fig. 13) is identical to that found in the structure of metavoltine, $Na_6K_2Fe^{2+}Fe^{3+}_6O_2(SO_4)_{12}\cdot 18H_2O$ (Giacovazzo et al. 1976). In fact, the structures of carlsonite and metavoltine are remarkably similar, as shown in Figure 12. Note that the placements of the NH_4 groups in the structure of carlsonite are similar to the placements of Na and K in the structure of metavoltine, providing further support for our assignments of the NH_4 sites. The same cluster is also found in the structure of Maus' salt, $K_5Fe^{3+}_3(SO_4)_6(OH)_2\cdot nH_2O$, and several related compounds (cf. Scordari et al. 1994).

Table 3a. Sample and crystal data for carlsonite[a]

Diffractometer	Rigaku R-Axis Rapid II	
X-ray radiation/power	Mo$K\alpha$ (λ = 0.71075 Å)/50 kV, 40 mA	
Temperature	298(2) K	
Structural formula	$(NH_4)_5Fe^{3+}_3O(SO_4)_6\cdot 7H_2O$	
Space group	$P\bar{1}$	
Unit-cell dimensions	a = 9.5927(2) Å	α = 93.250(7)°
	b = 9.7679(3) Å	β = 95.258(7)°
	c = 18.3995(13) Å	γ = 117.993(8)°
V	1506.15(16) Å^3	
Z	2	
Density (for above formula)	2.153 g/cm^3	
Absorption coefficient	1.968 mm^{-1}	
F(000)	998	
Crystal size	200 × 130 × 110 µm	
θ range	3.0 to 27.45°	
Index ranges	$-12 \le h \le 12$, $-12 \le k \le 12$, $-23 \le l \le 23$	
Reflections collected/unique	28480/6869; R_{int} = 0.017	
Reflections with $F_o > 4\sigma(F)$	6430	
Completeness to θ = 27.45°	99.7%	
Max. and min. transmission	0.813 and 0.694	
Refinement method	Full-matrix least-squares on F^2	
Parameters refined/restrained	71/517	
GoF	1.124	
Final R indices [$F_o > 4\sigma(F)$]	R_1 = 0.0297, wR_2 = 0.0812	
R indices (all data)	R_1 = 0.0314, wR_2 = 0.0826	
Largest diff. peak/hole	+0.94/–0.77 e/A^3	

[a] $R_{int} = \Sigma|F_o^2 - F_o^2(\text{mean})|/\Sigma[F_o^2]$. GoF = $S = \{\Sigma[w(F_o^2 - F_c^2)^2]/(n-p)\}^{1/2}$. $R_1 = \Sigma||F_o| - |F_c||/\Sigma|F_o|$. $wR_2 = \{\Sigma[w(F_o^2 - F_c^2)^2]/\Sigma[w(F_o^2)^2]\}^{1/2}$; $w = 1/[\sigma^2(F_o^2) + (aP)^2 + bP]$ where a is 0.0505, b is 1.0203, and P is $[2F_c^2 + \text{Max}(F_o^2,0)]/3$.

Table 3b. Sample and crystal data for huizingite-(Al)[a]

Diffractometer	Rigaku R-Axis Rapid II	
X-ray radiation/power	Mo$K\alpha$ (λ = 0.71075 Å)/50 kV, 40 mA	
Temperature	298(2) K	
Structural formula	$[(NH_4)_9(SO_4)_2][(Al_{1.72}Fe_{1.28})_3(SO_4)_6(OH)_2(H_2O)_4]$	
Space group	$P\bar{1}$	
Unit-cell dimensions	a = 9.7093(3) Å	α = 77.231(5)°
	b = 10.4341(3) Å	β = 74.860(5)°
	c = 10.7027(8) Å	γ = 66.104(5)°
V	948.73(9) Å^3	
Z	1	
Density (for above formula)	2.021 g/cm^3	
Absorption coefficient	1.113 mm^{-1}	
F(000)	597	
Crystal size	90 × 60 × 30 µm	
θ range	3.12 to 27.45°	
Index ranges	$-12 \le h \le 12$, $-13 \le k \le 13$, $-13 \le l \le 13$	
Reflections collected/unique	18529/4323; R_{int} = 0.046	
Reflections with $F_o > 4\sigma(F)$	3543	
Completeness to θ = 27.45°	99.6%	
Max. and min. transmission	0.967 and 0.906	
Refinement method	Full-matrix least-squares on F^2	
Parameters refined/restrained	342/50	
GoF	1.059	
Final R indices [$F_o > 4\sigma(F)$]	R_1 = 0.0399, wR_2 = 0.0874	
R indices (all data)	R_1 = 0.0519, wR_2 = 0.0925	
Largest diff. peak/hole	+0.40/–0.50 e/A^3	

[a] $R_{int} = \Sigma|F_o^2 - F_o^2(\text{mean})|/\Sigma[F_o^2]$. GoF = $S = \{\Sigma[w(F_o^2 - F_c^2)^2]/(n-p)\}^{1/2}$. $R_1 = \Sigma||F_o| - |F_c||/\Sigma|F_o|$. $wR_2 = \{\Sigma[w(F_o^2 - F_c^2)^2]/\Sigma[w(F_o^2)^2]\}^{1/2}$; $w = 1/[\sigma^2(F_o^2) + (aP)^2 + bP]$ where a is 0.0375, b is 1.0704, and P is $[2F_c^2 + \text{Max}(F_o^2,0)]/3$.

TABLE 4a. Atom coordinates and displacement parameters (Å^2) for carlsonite

	x/a	*y/b*	*z/c*	U_{eq}
Fe1	0.62121(3)	0.25279(3)	0.24651(2)	0.01520(7)
Fe2	0.36807(3)	0.39286(3)	0.26517(2)	0.01689(7)
Fe3	0.24002(3)	0.00884(3)	0.25780(2)	0.01645(7)
S1	0.42868(6)	–0.06325(6)	0.13719(3)	0.01942(11)
S2	0.71360(6)	0.54664(6)	0.36759(3)	0.01832(10)
S3	0.51278(6)	–0.00006(6)	0.36580(3)	0.01964(11)
S4	0.06836(6)	0.13994(6)	0.14676(3)	0.01828(10)
S5	0.59911(6)	0.49178(6)	0.13715(3)	0.02132(11)
S6	0.12297(6)	0.18539(6)	0.37145(3)	0.01986(11)
O1	0.4974(2)	–0.1674(2)	0.13588(11)	0.0371(4)
O2	0.3344(2)	–0.0787(3)	0.06780(10)	0.0440(5)
O3	0.55703(19)	0.10241(18)	0.15437(8)	0.0263(3)
O4	0.32513(18)	–0.10129(17)	0.19731(8)	0.0226(3)
O5	0.7032(3)	0.5393(2)	0.44527(10)	0.0418(4)
O6	0.8492(2)	0.6918(2)	0.35524(10)	0.0317(4)
O7	0.7256(2)	0.40985(19)	0.33607(9)	0.0298(4)
O8	0.5675(2)	0.54338(19)	0.32936(11)	0.0351(4)
O9	0.5916(2)	0.0827(2)	0.43761(9)	0.0355(4)
O10	0.4965(2)	–0.15715(19)	0.35909(9)	0.0313(4)
O11	0.60687(18)	0.08306(18)	0.30713(8)	0.0225(3)
O12	0.35299(19)	–0.0077(2)	0.35345(8)	0.0267(3)
O13	0.0973(3)	0.1789(2)	0.07287(9)	0.0405(4)
O14	–0.10093(18)	0.0754(2)	0.15429(10)	0.0295(3)
O15	0.1212(2)	0.02310(19)	0.16453(9)	0.0269(3)
O16	0.15765(18)	0.28191(17)	0.20106(9)	0.0244(3)
O17	0.5322(3)	0.4022(3)	0.06609(11)	0.0589(6)
O18	0.7109(2)	0.6528(2)	0.13069(12)	0.0401(4)
O19	0.4691(2)	0.4878(2)	0.17653(11)	0.0390(4)
O20	0.68350(19)	0.42422(19)	0.18223(9)	0.0274(3)
O21	0.1458(2)	0.1434(2)	0.44455(9)	0.0317(4)
O22	–0.0144(2)	0.2120(2)	0.36220(9)	0.0349(4)
O23	0.2705(2)	0.32705(19)	0.35946(8)	0.0279(3)
O24	0.09649(18)	0.05547(18)	0.31503(8)	0.0248(3)
O25	0.41093(16)	0.21995(16)	0.25570(7)	0.0161(3)
OW1	0.85062(18)	0.28090(18)	0.23993(9)	0.0228(3)
HW1a	0.904(3)	0.290(3)	0.2794(12)	0.027
HW1b	0.857(3)	0.219(3)	0.2110(13)	0.027
OW2	0.3064(2)	0.5696(2)	0.27352(10)	0.0319(4)
HW2a	0.249(3)	0.578(4)	0.2395(14)	0.038
HW2b	0.353(3)	0.655(3)	0.2965(15)	0.038
OW3	0.0645(2)	–0.2161(2)	0.26112(11)	0.0363(4)
HW3a	0.054(4)	–0.296(3)	0.2366(16)	0.044
HW3b	0.003(4)	–0.254(4)	0.2902(15)	0.044
OW4	0.0689(2)	0.5530(2)	0.17521(13)	0.0443(5)
HW4a	0.042(4)	0.587(4)	0.1395(16)	0.053
HW4b	0.003(4)	0.468(3)	0.1749(19)	0.053
OW5	0.8216(5)	0.3194(4)	0.05751(17)	0.0793(9)
HW5a	0.894(5)	0.323(6)	0.024(2)	0.095
HW5b	0.746(4)	0.237(5)	0.025(2)	0.095
OW6	0.1324(8)	0.5631(6)	0.4345(4)	0.171(3)
HW6a	0.037(9)	0.507(10)	0.454(4)	0.205
HW6b	0.100(9)	0.548(10)	0.3879(19)	0.205
OW7	0.0086(3)	0.2942(3)	–0.07344(12)	0.0488(5)
HW7a	0.079(3)	0.283(4)	–0.089(2)	0.059
HW7b	–0.069(3)	0.211(3)	–0.076(2)	0.059
N1	0.4767(3)	0.2788(3)	0.50578(12)	0.0367(5)
HN1a	0.380(2)	0.263(4)	0.4955(16)	0.044
HN1b	0.538(3)	0.370(3)	0.4912(16)	0.044
HN1c	0.497(4)	0.279(3)	0.5524(11)	0.044
HN1d	0.497(4)	0.211(3)	0.4809(15)	0.044
N2	0.2935(3)	0.1274(3)	–0.02010(11)	0.0337(4)
HN2a	0.314(3)	0.065(3)	0.0086(14)	0.040
HN2b	0.223(3)	0.142(3)	0.0058(15)	0.040
HN2c	0.375(3)	0.211(3)	–0.0159(16)	0.040
HN2d	0.242(3)	0.072(3)	–0.0594(12)	0.040
N3	0.2574(3)	0.5122(3)	0.05027(14)	0.0462(6)
HN3a	0.210(4)	0.559(4)	0.0251(16)	0.055
HN3b	0.326(3)	0.508(4)	0.0219(16)	0.055
HN3c	0.317(3)	0.587(3)	0.0872(14)	0.055
HN3d	0.188(3)	0.432(3)	0.0637(18)	0.055
N4	0.1104(3)	–0.1644(3)	0.47709(12)	0.0364(5)
HN4a	0.197(3)	–0.131(3)	0.5133(13)	0.044
HN4b	0.101(4)	–0.249(3)	0.4560(15)	0.044
HN4c	0.131(4)	–0.092(3)	0.4508(14)	0.044
HN4d	0.029(3)	–0.185(3)	0.5018(15)	0.044
N5	0.7340(2)	–0.1376(2)	0.25778(11)	0.0249(4)
HN5a	0.818(2)	–0.075(3)	0.2489(14)	0.030
HN5b	0.733(3)	–0.199(3)	0.2887(13)	0.030
HN5c	0.665(3)	–0.186(3)	0.2213(11)	0.030
HN5d	0.692(3)	–0.088(3)	0.2820(13)	0.030

(Table 4b on next page)

Huizingite-(Al)

Huizingite-(Al) is also a bipartite structure. The $[(Al,Fe^{3+})_3(OH)_2(H_2O)_4(SO_4)_6]^{5-}$ cluster defines the structural unit and the interstitial complex has the formula $[(NH_4)_9(SO_4)_2]^{5+}$. The atomic arrangement of huizingite-(Al) is depicted in Figure 14 and the structural unit is compared to that of carlsonite in Figure 13.

The structural unit in the structure of huizingite-Al is a cluster containing the same polyhedral components, three $M^{3+}O_6$ octahedra (M^{3+} = Fe or Al) and six SO_4 groups, that make up the cluster in the structure of carlsonite; however, the polyhedra are linked quite differently. In the carlsonite cluster, three FeO_6 octahedra share a common vertex, while in the huizingite-(Al) cluster, three $(Al,Fe)O_6$ octahedra form an abbreviated corner-linked chain. The polyhedral cluster in the huizingite-(Al) structure is unique, but has the same topology as a segment of the $[Fe^{3+}(SO_4)_3]^{3-}$ polyhedral chain in the structure of sideronatrite (Scordari and Ventruti 2009).

NH_4-O bonding

The NH_4-O bond lengths in the structure of carlsonite vary from 2.796 to 3.380 Å, corresponding to coordinations of 7, 6, 8, 7, and 8 for $NH_4$1, $NH_4$2, $NH_4$3, $NH_4$4, and $NH_4$5, respectively. Those in huizingite-(Al) vary from 2.729 to 3.281 Å, corresponding to coordinations of 7, 7, 7, 8, and 6 for $NH_4$1, $NH_4$2, $NH_4$3, $NH_4$4, and $NH_4$5, respectively. Khan and Baur (1972) surveyed NH_4-containing structures and noted that NH_4-O coordinations vary from 4 to 9; for small (4 or 5) coordinations, the NH_4 group behaves more like a conventional hydrogen-bond donor, forming nearly linear N–H···O bonds; for higher coordinations, the NH_4 group behaves more like an alkali cation, with either the NH_4 group exhibiting orientational disorder or the H bonds being polyfurcated. In a study of the crystal structure of hannayite, $Mg_3(NH_4)_2(HPO_4)_4{\cdot}8H_2O$, Catti and Franchini-Angela (1976) described the hybrid (or dual) bonding behavior of the NH_4^+ group between an ordered hydrogen-bond donor and a strongly electropositive large alkali-like cation. They observed that this dual behavior for NH_4^+ is apparently quite common. The dual-bonding behavior of NH_4 is clearly observed in the structures of carlsonite and huizingite-(Al) (Table 6); with the exceptions of HN5a in carlsonite and HN3d in huizingite-(Al), each of the H atoms associated with the NH_4 groups forms a single short, nearly linear hydrogen bond to an O atom, while other NH_4-O bonds are more appropriately regarded as electrostatic in nature. It is noteworthy that the dual-bonding behavior of NH_4 was also reported in pyracmonite, $(NH_4)_3Fe^{3+}(SO_4)_3$ (Demartin et al. 2010), a mineral that is also found in the Huron River burn site mineral suite.

Table 4b. Atom coordinates and displacement parameters (Å²) for huizingite-(Al)

	x/a	*y/b*	*z/c*	U_{eq}
Al1	0.5	0.5	0.0	0.0184(3)
Al2	0.40551(6)	0.74296(5)	0.21230(5)	0.01774(18)
S1	0.37237(7)	0.24458(7)	0.06816(6)	0.02067(16)
S2	0.19631(8)	0.76866(7)	0.01591(7)	0.02286(16)
S3	0.69632(8)	0.54010(7)	0.34623(7)	0.02388(16)
S4	0.82969(8)	0.87469(8)	0.46665(7)	0.02857(18)
O1	0.2184(2)	0.2426(2)	0.0949(2)	0.0316(5)
O2	0.4652(2)	0.1410(2)	0.15867(19)	0.0298(5)
O3	0.3605(2)	0.3897(2)	0.07501(19)	0.0273(4)
O4	0.5546(2)	0.7897(2)	0.06772(18)	0.0270(4)
O5	0.1315(3)	0.8847(2)	–0.0795(2)	0.0426(6)
O6	0.0895(2)	0.7015(3)	0.0888(2)	0.0421(6)
O7	0.3338(2)	0.6619(2)	–0.05358(19)	0.0277(4)
O8	0.2471(2)	0.8229(2)	0.1065(2)	0.0300(5)
O9	0.8258(3)	0.5652(3)	0.2550(3)	0.0496(6)
O10	0.7139(3)	0.5238(2)	0.4811(2)	0.0409(6)
O11	0.6796(3)	0.4144(2)	0.3211(2)	0.0402(6)
O12	0.5535(2)	0.6654(2)	0.3284(2)	0.0289(5)
O13	0.8548(4)	0.7691(3)	0.5804(3)	0.0744(10)
O14	0.6914(3)	0.8920(3)	0.4237(2)	0.0486(6)
O15	0.9596(3)	0.8390(4)	0.3573(3)	0.0640(9)
O16	0.8101(3)	0.0103(3)	0.5023(2)	0.0485(6)
OH1	0.4586(2)	0.5597(2)	0.16627(19)	0.0228(4)
H1	0.523(3)	0.503(3)	0.203(3)	0.027
OW1	0.3499(3)	0.9294(2)	0.2612(2)	0.0303(5)
HW1a	0.295(3)	0.946(4)	0.333(3)	0.036
HW1b	0.386(4)	0.988(3)	0.235(3)	0.036
OW2	0.2507(2)	0.7242(2)	0.3647(2)	0.0322(5)
HW2a	0.276(4)	0.664(3)	0.422(3)	0.039
HW2b	0.159(3)	0.756(3)	0.366(3)	0.039
N1	0.4800(3)	0.7877(3)	0.6057(3)	0.0382(6)
HN1a	0.555(3)	0.798(3)	0.547(3)	0.046
HN1b	0.486(4)	0.794(3)	0.686(2)	0.046
HN1c	0.393(3)	0.859(3)	0.586(3)	0.046
HN1d	0.465(4)	0.709(3)	0.609(3)	0.046
N2	0.0275(4)	0.8436(4)	0.7176(3)	0.0474(8)
HN2a	0.107(3)	0.765(3)	0.716(4)	0.057
HN2b	0.008(4)	0.890(3)	0.783(3)	0.057
HN2c	–0.056(3)	0.835(4)	0.712(3)	0.057
HN2d	0.054(4)	0.903(3)	0.646(3)	0.057
N3	0.1115(4)	0.5045(4)	0.3225(3)	0.0516(8)
HN3a	0.142(4)	0.517(4)	0.389(3)	0.062
HN3b	0.127(4)	0.409(2)	0.338(4)	0.062
HN3c	0.019(3)	0.552(3)	0.318(4)	0.062
HN3d	0.178(4)	0.515(4)	0.251(3)	0.062
N4	0.2297(3)	0.1194(3)	0.8502(3)	0.0363(6)
HN4a	0.261(4)	0.126(3)	0.765(2)	0.044
HN4b	0.230(4)	0.039(2)	0.888(3)	0.044
HN4c	0.134(2)	0.182(3)	0.865(3)	0.044
HN4d	0.286(3)	0.150(3)	0.881(3)	0.044
N5	0.0000	0.5000	0.0000	0.0552(13)
HN5a	0.044(10)	0.555(9)	0.013(10)	0.066
HN5b	0.061(7)	0.419(5)	0.039(6)	0.066
HN5c	0.059(8)	0.494(9)	–0.081(4)	0.066

Note: Site occupancies: Al1 = Al/Fe 0.597/0.403(5), Al2 = Al/Fe 0.562/0.438(4), HN5A = 0.50(9), HN5B = 0.69(8), HN5C = 0.58(9)

Lewis acidity-basicity

Hawthorne and Schindler (2008) noted that the strengths of the relatively weak bonds between the strongly bonded *structural unit* (SU) and the *interstitial complex* (IC) usually control the stability of a structure. Furthermore, they pointed out that the interaction between the typically anionic SU and the typically cationic IC can be examined using the Principle of Correspondence of Lewis acidity-basicity. The Lewis basicity (LB) of the SU reflects its capacity to donate electron density and the Lewis acidity (LA) of the IC reflects its capacity to accept electron density; these quantities are essentially equivalent to bond valence and are expressed in valence units (v.u.). The Principle of Correspondence states that, when the LA closely

Table 5a. Selected bond distances (Å) for carlsonite

$NH_4$1-O5	2.830(3)	S1-O1	1.4492(17)	Fe1-O25	1.9136(13)
$NH_4$1-O10	2.858(3)	S1-O2	1.4522(18)	Fe1-O20	1.9937(15)
$NH_4$1-O21	2.886(3)	S1-O3	1.4949(16)	Fe1-O11	2.0087(14)
$NH_4$1-O9	2.902(3)	S1-O4	1.5000(15)	Fe1-O7	2.0100(16)
$NH_4$1-O5	3.151(3)	<S1-O>	1.4741	Fe1-O3	2.0220(15)
$NH_4$1-OW6	3.355(6)			Fe1-OW1	2.1019(15)
$NH_4$1-O23	3.380(3)	S2-O5	1.4452(17)	<Fe1-O>	2.0083
<$NH_4$1-O>	3.052	S2-O6	1.4537(17)		
		S2-O7	1.4844(16)	Fe2-O25	1.9192(13)
$NH_4$2-O2	2.796(3)	S2-O8	1.4952(16)	Fe2-O8	1.9911(17)
$NH_4$2-O17	2.836(3)	<S2-O>	1.4696	Fe2-O16	2.0014(15)
$NH_4$2-O13	2.847(3)			Fe2-O19	2.0191(17)
$NH_4$2-O14	2.934(3)	S3-O9	1.4467(17)	Fe2-O23	2.0390(16)
$NH_4$2-O1	2.976(3)	S3-O10	1.4643(17)	Fe2-OW2	2.0735(16)
$NH_4$2-O18	3.052(3)	S3-O11	1.4930(15)	<Fe2-O>	2.0072
<$NH_4$2-O>	2.907	S3-O12	1.4944(16)		
		<S3-O>	1.4746	Fe3-O25	1.9465(14)
$NH_4$3-OW5	2.911(4)			Fe3-O4	1.9793(14)
$NH_4$3-O13	2.951(3)	S4-O13	1.4489(17)	Fe3-O24	2.0030(15)
$NH_4$3-O17	2.961(4)	S4-O14	1.4642(16)	Fe3-O15	2.0200(15)
$NH_4$3-OW7	3.016(3)	S4-O15	1.4907(15)	Fe3-O12	2.0360(15)
$NH_4$3-O19	3.038(3)	S4-O16	1.4920(15)	Fe3-OW3	2.0560(17)
$NH_4$3-O1	3.096(3)	<S4-O>	1.4740	<Fe2-O>	2.0068
$NH_4$3-OW4	3.170(4)				
$NH_4$3-O17	3.278(4)	S5-O17	1.4410(21)	**Hydrogen bonds**	
<$NH_4$3-O>	3.053	S5-O18	1.4491(18)	OW1···O22	2.765(2)
		S5-O19	1.4846(17)	OW1···O14	2.717(2)
$NH_4$4-OW6	2.838(5)	S5-O20	1.4897(16)	OW2···OW4	2.711(3)
$NH_4$4-O9	2.858(3)	<S5-O>	1.4661	OW2···O10	2.713(3)
$NH_4$4-O6	2.930(3)			OW3···OW4	2.699(3)
$NH_4$4-O21	2.966(3)	S6-O21	1.4555(16)	OW3···O6	2.676(2)
$NH_4$4-O21	3.042(3)	S6-O22	1.4557(16)	OW4···OW7	2.719(3)
$NH_4$4-O22	3.172(3)	S6-O23	1.4902(17)	OW4···OW1	2.908(3)
$NH_4$4-O12	3.310(3)	S6-O24	1.5007(15)	OW5···OW7	3.198(4)
<$NH_4$4-O>	3.017	<S6-O>	1.4755	OW5···O2	2.921(4)
				OW6···none	
$NH_4$5-O14	2.894(3)			OW6···none	
$NH_4$5-O1	2.939(3)			OW7···O18	2.808(3)
$NH_4$5-O18	2.940(3)			OW7···O2	2.976(3)
$NH_4$5-O6	2.986(3)				
$NH_4$5-O10	3.018(3)				
$NH_4$5-O11	3.067(2)				
$NH_4$5-O24	3.116(3)				
$NH_4$5-O8	3.189(3)				
<$NH_4$5-O>	3.019				

Table 5b. Selected bond distances (Å) for huizingite-(Al)

$NH_4$1-O14	2.824(4)	$NH_4$4-O14	2.847(4)	S1-O1	1.455(2)
$NH_4$1-O11	2.957(4)	$NH_4$4-O5	2.860(4)	S1-O2	1.457(2)
$NH_4$1-O2	3.008(4)	$NH_4$4-O6	2.883(4)	S1-O3	1.488(2)
$NH_4$1-O14	3.056(4)	$NH_4$4-O4	2.999(3)	S1-O4	1.4938(19)
$NH_4$1-O10	3.081(4)	$NH_4$4-O15	3.092(4)	<Si1-O>	1.473
$NH_4$1-O16	3.086(4)	$NH_4$4-O2	3.100(3)		
$NH_4$1-O12	3.281(4)	$NH_4$4-O9	3.103(4)	S2-O5	1.441(2)
<$NH_4$1-O>	3.042	$NH_4$4-O1	3.122(3)	S2-O6	1.449(2)
		<$NH_4$4-O>	3.001	S2-O7	1.490(2)
$NH_4$2-O5	2.797(4)			S2-O8	1.491(2)
$NH_4$2-O13	2.902(4)	$NH_4$5-O1(×2)	2.837(2)	<Si2-O>	1.468
$NH_4$2-O16	2.962(4)	$NH_4$5-O9(×2)	2.872(3)		
$NH_4$2-O1	2.996(4)	$NH_4$5-O6(×2)	2.979(2)	S3-O9	1.454(2)
$NH_4$2-O11	3.030(4)	<$NH_4$5-O>	2.896	S3-O10	1.462(2)
$NH_4$2-O16	3.254(4)			S3-O11	1.473(2)
$NH_4$2-O15	3.277(5)	Al1-OH1(×2)	1.9051(19)	S3-O12	1.493(2)
<$NH_4$2-O>	3.031	Al1-O7(×2)	1.906(2)	<Si3-O>	1.471
		Al1-O3(×2)	2.0225(19)		
$NH_4$3-O13	2.729(4)	<Al1-O>	1.945	S4-O13	1.449(3)
$NH_4$3-O9	2.836(4)			S4-O14	1.462(2)
$NH_4$3-O6	2.860(4)	Al2-OH1	1.9107(19)	S4-O15	1.463(3)
$NH_4$3-O10	2.926(4)	Al2-OW2	1.943(2)	S4-O16	1.472(2)
$NH_4$3-O3	3.163(4)	Al2-O4	1.9480(19)	<Si4-O>	1.462
$NH_4$3-OW2	3.251(4)	Al2-O8	1.948(2)		
$NH_4$3-O15	3.258(5)	Al2-OW1	1.950(2)	**Hydrogen bonds**	
<$NH_4$3-O>	3.003	Al2-O12	1.952(2)	OH1···O11	2.786(3)
		<Al2-O>	1.942	OW1···O16	2.660(3)
				OW1···O2	2.761(3)
				OW2···O10	2.688(3)
				OW2···O15	2.601(3)

Table 6a. Bond distances and angles for N-H-O bonds in carlsonite

N-H···O	*d*(N-H)	*d*(H····O)	*d*(N-O)	<N-H···O	NH_4···O bonding[a]
N1-HN1a···O21	0.87(2)	2.08(2)	2.886(3)	155(3)	hydrogen bond
N1-HN1a···O5	0.87(2)	2.63(3)	3.151(3)	120(2)	electrostatic bond
N1-HN1a···O23	0.87(2)	2.84(3)	3.380(3)	122(2)	electrostatic bond
N1-HN1b···O5	0.88(2)	1.97(2)	2.830(3)	163(3)	hydrogen bond
N1-HN1b···OW6	0.88(2)	3.07(3)	3.357(6)	101(2)	electrostatic bond
N1-HN1c···O10	0.86(2)	2.09(2)	2.858(3)	149(3)	hydrogen bond
N1-HN1d···O9	0.89(2)	2.02(2)	2.902(3)	168(3)	hydrogen bond
N2-HN2a···O2	0.91(2)	1.89(2)	2.796(3)	174(3)	hydrogen bond
N2-HN2b···O13	0.92(2)	1.93(2)	2.847(3)	172(3)	hydrogen bond
N2-HN2c···O17	0.82(2)	2.16(2)	2.836(3)	140(3)	hydrogen bond
N2-HN2c···O1	0.82(2)	2.72(3)	2.976(3)	100(2)	electrostatic bond
N2-HN2c···O18	0.82(2)	2.82(3)	3.052(3)	99(2)	electrostatic bond
N2-HN2d···O14	0.84(2)	2.10(2)	2.934(3)	176(3)	hydrogen bond
N3-HN3a···OW5	0.90(2)	2.07(2)	2.911(4)	156(3)	hydrogen bond
N3-HN3b···O17	0.89(2)	2.16(3)	2.961(4)	148(3)	hydrogen bond
N3-HN3b···O17	0.89(2)	2.71(3)	3.278(4)	123(3)	electrostatic bond
N3-HN3c···O1	0.90(2)	2.26(2)	3.096(3)	154(3)	hydrogen bond
N3-HN3c···O19	0.90(2)	2.61(3)	3.038(3)	110(2)	electrostatic bond
N3-HN3d···O13	0.82(2)	2.23(2)	2.951(3)	147(3)	hydrogen bond
N3-HN3d···OW7	0.82(2)	2.79(3)	3.016(3)	98(2)	electrostatic bond
N3-HN3d···OW4	0.82(2)	2.88(3)	3.170(4)	103(2)	electrostatic bond
N4-HN4a···O9	0.93(2)	1.97(2)	2.858(3)	160(3)	hydrogen bond
N4-HN4b···OW6	0.86(2)	2.01(2)	2.839(5)	161(3)	hydrogen bond
N4-HN4b···O6	0.86(2)	2.71(3)	2.930(3)	96(2)	electrostatic bond
N4-HN4c···O21	0.84(2)	2.24(2)	2.966(3)	144(3)	hydrogen bond
N4-HN4c···O12	0.84(2)	2.76(3)	3.310(3)	124(2)	electrostatic bond
N4-HN4d···O21	0.89(2)	2.20(2)	3.042(3)	158(3)	hydrogen bond
N4-HN4d···O22	0.89(2)	2.54(3)	3.172(3)	129(2)	electrostatic bond
N5-HN5a···O14	0.79(2)	2.30(2)	2.894(3)	133(2)	electrostatic bond
N5-HN5a···O24	0.79(2)	2.51(2)	3.116(3)	135(2)	electrostatic bond
N5-HN5b···O6	0.85(2)	2.21(2)	2.986(3)	152(2)	hydrogen bond
N5-HN5b···O8	0.85(2)	2.47(2)	3.189(3)	143(2)	electrostatic bond
N5-HN5c···O1	0.84(2)	2.22(2)	2.939(3)	144(2)	hydrogen bond
N5-HN5c···O18	0.84(2)	2.43(2)	2.940(3)	120(2)	electrostatic bond
N5-HN5d···O11	0.89(2)	2.22(2)	3.067(2)	159(2)	hydrogen bond
N5-HN5d···O10	0.89(2)	2.32(2)	3.018(3)	136(2)	electrostatic bond

[a] The NH_4···O bond is interpreted as being predominantly an ordered hydrogen bond if *d*(H···O) is short (<2.27 Å) and <N-H···O is large (>140°).

Table 6b. Bond distances and angles for N-H-O bonds in huizingite-(Al)

N-H···O	*d*(N-H)	*d*(H···O)	*d*(N-O)	<N-H···O	NH_4···O bonding[a]
N1-HN1a···O14	0.86(2)	2.00(2)	2.824(4)	159(3)	hydrogen bond
N1-HN1b···O2	0.90(2)	2.15(2)	3.008(4)	161(3)	hydrogen bond
N1-HN1c···O14	0.91(2)	2.37(3)	3.056(4)	132(3)	electrostatic bond
N1-HN1c···O16	0.91(2)	2.20(2)	3.086(4)	163(3)	hydrogen bond
N1-HN1d···O10	0.88(2)	2.66(3)	3.081(4)	110(2)	electrostatic bond
N1-HN1d···O11	0.88(2)	2.16(2)	2.957(4)	149(3)	hydrogen bond
N2-HN2a···O11	0.87(2)	2.17(2)	3.030(4)	170(3)	hydrogen bond
N2-HN2b···O5	0.88(2)	2.10(3)	2.797(4)	135(3)	hydrogen bond
N2-HN2c···O1	0.87(2)	2.45(3)	2.996(4)	121(3)	electrostatic bond
N2-HN2c···O13	0.87(2)	2.18(3)	2.902(4)	140(3)	hydrogen bond
N2-HN2c···O16	0.87(2)	2.80(3)	3.254(4)	114(3)	electrostatic bond
N2-HN2d···O15	0.93(2)	2.63(3)	3.277(5)	127(3)	electrostatic bond
N2-HN2d···O16	0.93(2)	2.08(2)	2.962(4)	160(3)	hydrogen bond
N3-HN3a···O10	0.89(2)	2.09(2)	2.926(4)	157(3)	hydrogen bond
N3-HN3a···OW2	0.89(2)	2.71(3)	3.251(4)	121(3)	electrostatic bond
N3-HN3b···O13	0.93(2)	1.83(2)	2.729(4)	163(3)	hydrogen bond
N3-HN3c···O9	0.84(2)	2.10(3)	2.836(4)	146(3)	hydrogen bond
N3-HN3c···O15	0.84(2)	2.91(4)	3.258(5)	107(3)	electrostatic bond
N3-HN3d···O3	0.89(2)	2.42(3)	3.163(4)	142(3)	electrostatic bond
N3-HN3d···O6	0.89(2)	2.34(3)	2.860(4)	118(3)	electrostatic bond
N4-HN4a···O14	0.88(2)	1.98(2)	2.847(4)	166(3)	hydrogen bond
N4-HN4a···O15	0.88(2)	2.66(3)	3.092(4)	112(2)	electrostatic bond
N4-HN4b···O5	0.85(2)	2.11(2)	2.860(4)	148(3)	hydrogen bond
N4-HN4b···O2	0.85(2)	2.77(3)	3.100(3)	105(2)	electrostatic bond
N4-HN4c···O6	0.89(2)	2.00(2)	2.883(4)	171(3)	hydrogen bond
N4-HN4c···O9	0.89(2)	2.80(3)	3.103(4)	102(2)	electrostatic bond
N4-HN4d···O1	0.89(2)	2.51(3)	3.122(3)	126(2)	electrostatic bond
N4-HN4d···O4	0.89(2)	2.11(2)	2.999(3)	172(3)	hydrogen bond
N5-HN5a···O6	0.90(3)	2.11(4)	2.979(2)	163(9)	hydrogen bond
N5-HN5b···O1	0.90(3)	1.95(3)	2.837(2)	170(7)	hydrogen bond
N5-HN5c···O9	0.90(3)	1.99(4)	2.872(3)	164(8)	hydrogen bond

[a] The NH_4···O bond is interpreted as being predominantly an ordered hydrogen bond if *d*(H···O) is short (<2.27 Å) and <N-H···O is large (>140°).

matches the LB, a stable structure will form.

Using the approach detailed by Hawthorne and Schindler (2008), the characteristic range in LB for the SU in carlsonite can be calculated as follows: the effective charge (EC) = the formal charge of the SU less the charge transferred by hydrogen bonding (6 H bonds) = $5^- - 6 \times 0.2 = 6.2^-$. The charge deficiency per anion (CDA) = EC per O atom (28 O atoms) = $6.2^-/28 = 0.22^-$. The range in the average number of bonds ($<NB_{in}>$) from the IC to O atoms in the SU obtained from Figure 8c in Hawthorne and Schindler (2008) $<NB_{in}> = 0.95–1.95$. The range in total number of bonds (RB) to the SU = $<NB_{in}> \times$ number of O atoms = $(0.95–1.95) \times 28 = 26.6–54.46$. The range in LB of the SU of carlsonite = EC/RB = 6.2/(26.6–54.46) = 0.23–0.11 v.u. For huizingite-(Al), the same procedure was used; however, it is worth noting that the unconnected SO_4 group, included as part of the IC, must be considered as part of the SU for the purpose of computing the LB because of the unconnected SO_4 group's strong internal bonding. The resulting range in LB for the SU in huizingite-(Al) was calculated to be 0.20–0.12 v.u.

Previous studies of Lewis acidity have largely overlooked the NH_4^+ group. In fact, prior listings of Lewis acid strengths for cations (cf. Hawthorne and Schindler 2008; Hawthorne 2012) do not include the NH_4^+ group. For purposes of calculating the LA of the IC in NH_4 phases, the distinction between hydrogen bonds and electrostatic bonds, discussed earlier, does not seem pertinent and the NH_4^+ group is probably best treated as a normal cation. The LA of the IC in carlsonite and huizingite-(Al) is computed as the formal charge of an NH_4^+ group (+1) divided by the average number of bonds emanating from each of the NH_4^+ groups, modified by any transformer H_2O groups. [For an explanation of transformer H_2O groups, the reader is referred to Hawthorne and Schindler (2008).] The calculated LA of the IC in carlsonite is 0.13 v.u. and in huizingite-(Al) is 0.14 v.u. In both cases, the principle of correspondence of Lewis acidity-basicity holds. Furthermore, the fact that in both cases the match occurs at the lower range of Lewis basicity is an indication that the environment in which these phases formed was not highly acidic.

Finally, it is worth considering the typical or average value of Lewis acid strength that should be attributed to the NH_4^+ cation, in general. The 0.13–0.14 v.u. values noted above for carlsonite and huizingite-(Al) correspond to average coordination numbers (CN) in the 7 to 8 range. It is well known that NH_4^+ forms many oxysalts that are isostructural with corresponding K^+ salts (cf. Khan and Baur 1972). The most common CN for K^+ is 8, which corresponds to a Lewis acid strength of 0.125 v.u. Indeed, Brown (1981) provided a Lewis acid strength of 0.13 v.u. for K^+ and this has been used by subsequent workers. Consequently, we suggest that 0.13 v.u. be used as the characteristic Lewis acid strength for NH_4^+, in most cases (7 to 8 CN); however, this value is probably not appropriate for those structures in which NH_4^+ has small (4 or 5) CN. For example, NH_4^+ has an average CN of 4 in $(NH_4)_3PO_4 \cdot 3H_2O$ (Mootz and Wunderlich 1970), with each of three distinct NH_4^+ groups forming four hydrogen bonds to O atoms of PO_4^{3-} groups (which constitute the structural unit). The PO_4^{3-} oxyanion has a characteristic Lewis basicity of 0.25 v.u. (cf. Hawthorne and Schindler 2008). In this structure, and others in which NH_4^+ has a CN of 4, it seems more appropriate to assign it a Lewis acid strength of 0.25 v.u. (charge/CN).

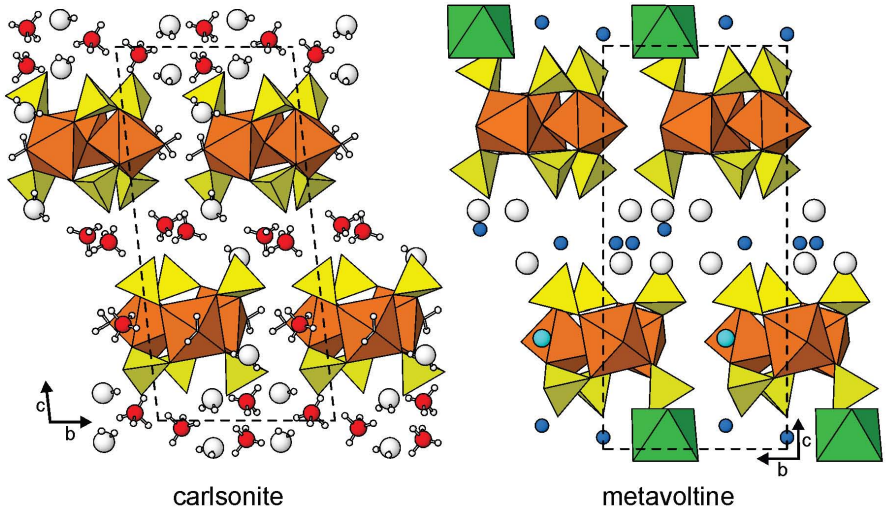

FIGURE 12. Atomic arrangements of carlsonite and metavoltine, viewed down [100]. $Fe^{3+}O_6$ octahedra are orange, $Fe^{2+}O_6$ octahedra are green, SO_4 tetrahedra are yellow, K atoms are light blue spheres, Na atoms are dark blue spheres, N atoms are red spheres, O atoms of isolated H_2O groups are large white spheres, and H atoms are small white spheres. N-H and O-H bonds are shown as sticks. Unit cells are shown with dashed lines.

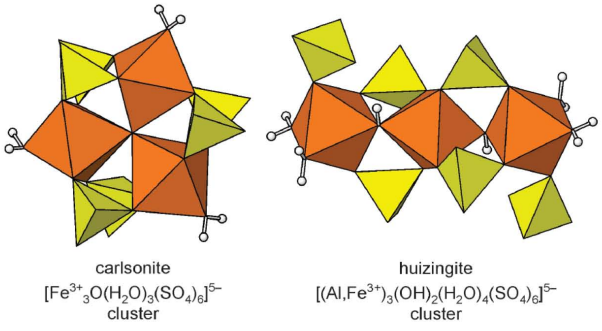

FIGURE 13. The structural units in carlsonite and huizingite-(Al). $Fe^{3+}O_6$ and AlO_6 octahedra are orange, SO_4 tetrahedra are yellow.

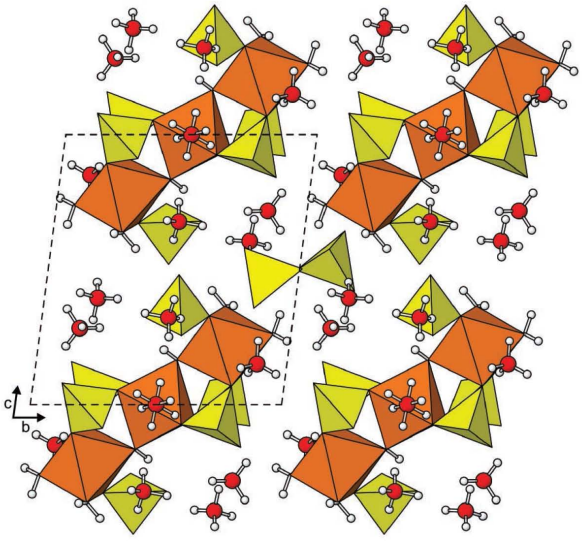

FIGURE 14. Atomic arrangement of huizingite-(Al) viewed down [100]. The structural components are as described in Figures 12 and 13. Note the disordered $NH_4$5 group on the center of symmetry at (0,½,0).

Relation of the structures to paragenesis

In a series of papers, Scordari and coworkers examined the structures and stabilities of some hydrated alkali iron sulfates (see Scordari et al. 1994, and references therein). These featured, in particular, phases containing the same $[Fe^{3+}{}_3O(H_2O)_3(SO_4)_6]^{5-}$ cluster that is found in carlsonite and metavoltine. They showed that these compounds gradually alter through dehydration to form phases with the ferrinatrite, $Na_3Fe(SO_4)_3 \cdot 3H_2O$, structure and that the transformation involves the rearrangement of the $[Fe^{3+}{}_3O(H_2O)_3(SO_4)_6]^{5-}$ clusters into chains of composition $[Fe^{3+}(SO_4)_3]^{3-}$. Compounds containing Na^+, K^+, and H_3O^+ were examined; however, phases containing NH_4^+ were not considered. Interestingly, as noted above, the huizingite-(Al) cluster is essentially a segment of a sideronatrite polyhedral chain.

IMPLICATIONS

The close structural relationship between carlsonite and metavoltine is intriguing considering that metavoltine is a widely distributed mineral occurring as an alteration product of pyrite in arid climates, as a fumarolic sublimate and solfataric precipitate, as a post-mining product, and as a coal-fire sublimate. The last of these modes of occurrence, whether of natural or anthropogenic origin, is similar to that at the Huron River burn site. Ammonium-bearing phases are typical of coal-fire occurrences [e.g., the burning coal dumps of the Upper Silesian Coal Basin (Parafiniuk and Kruszewski 2009) and the burning Anna I coal mine dump, Alsdorf, Germany (Witzke et al. 2015)] and can occur, as well, in other types of deposits; yet an ammonium analog of metavoltine has not been reported, either as a natural or synthetic phase; although Wendlandt and Harrison (2006) did report a NH_4-bearing metavoltine as a precipitate associated with uranium mill tailings disposal cells at the White Mesa Mill in

TABLE 7a. Bond-valence analysis for carlsonite

	$NH_4$1	$NH_4$2	$NH_4$3	$NH_4$4	$NH_4$5	Fe1	Fe2	Fe3	S1	S2	S3	S4	S5	S6	Hydrogen bonds	Σ
O1		0.13	0.10		0.15				1.60							1.98
O2		0.21							1.59						+0.14, +0.11	2.05
O3						0.49			1.42							1.91
O4								0.55	1.40							1.95
O5	0.20, 0.08									1.62						1.90
O6				0.15	0.13					1.58					+0.21	2.07
O7						0.51				1.46						1.97
O8					0.07		0.53			1.42						2.02
O9	0.16			0.18							1.61					1.95
O10	0.18				0.12						1.54				+0.20	2.04
O11					0.10	0.51					1.42					2.03
O12				0.05				0.47			1.42					1.94
O13		0.19	0.14									1.61				1.94
O14		0.15			0.16							1.54			+0.20	2.05
O15								0.49				1.43				1.92
O16							0.52					1.43				1.95
O17		0.19	0.14, 0.06										1.64			2.03
O18		0.11			0.15								1.60		+0.18	2.04
O19			0.11				0.49						1.46			2.06
O20						0.53							1.44			1.97
O21	0.17			0.14, 0.11										1.58		2.00
O22				0.08										1.58	+0.19	1.85
O23	0.04						0.47							1.44		1.95
O24					0.09			0.52						1.40		2.01
O25						0.66	0.65	0.60								1.91
OW1						0.40									–0.19, –0.20, +0.14	0.15
OW2							0.43								–0.20, –0.20	0.03
OW3								0.45							–0.20, –0.21	0.04
OW4			0.08												–0.20, –0.14, +0.20, +0.20	0.14
OW5			0.16												–0.00, –0.14	0.02
OW6	0.05			0.19											–0.00, –0.00	0.24
OW7			0.12												–0.18, –0.11, +0.20	0.03
Σ	0.68	0.98	0.61	0.70	0.67	3.10	3.09	3.08	6.01	6.08	5.99	6.01	6.14	6.00		

Notes: Values are expressed in valence units = NH_4^+-O bond strengths from Garcia-Rodriguez et al. (2000); Fe^{3+}-O bond strengths from Brown and Altermatt (1985); Si^{4+}-O bond strengths from Brese and O'Keeffe (1991).

TABLE 7b. Bond-valence analysis for huizingite-(Al)

	$NH_4$1	$NH_4$2	$NH_4$3	$NH_4$4	$NH_4$5	Al1	Al2	S1	S2	S3	S4	Hydrogen bonds	Σ
O1		0.12		0.09	$0.19^{\times 2\rightarrow}$			1.58					1.98
O2	0.12			0.09				1.57				+0.19	1.97
O3			0.08			$0.40^{\times 2\rightarrow}$		1.44					1.92
O4				0.12			0.49	1.42					2.03
O5		0.21		0.18					1.64				2.03
O6			0.18	0.17	$0.13^{\times 2\rightarrow}$				1.60				2.08
O7						$0.55^{\times 2\rightarrow}$			1.44				1.99
O8							0.49		1.43				1.92
O9			0.19	0.09	$0.17^{\times 2\rightarrow}$					1.58			2.03
O10	0.10		0.15							1.55		+0.21	2.01
O11	0.14	0.11								1.50		+0.18	1.93
O12	0.06						0.49			1.42			1.97
O13		0.16	0.26								1.60		2.02
O14	0.20, 0.11			0.19							1.55		2.05
O15		0.06	0.06	0.10							1.55	+0.24	2.01
O16	0.10	0.14, 0.06									1.51	+0.22	2.03
OH						$0.55^{\times 2\rightarrow}$	0.55					–0.18	0.92
OW1							0.49					–0.22, –0.19	0.08
OW2							0.50					–0.21, –0.24	0.05
Σ	0.83	0.86	0.92	1.03	0.98	2.99	3.01	6.01	6.11	6.05	6.21		

Notes: Values are expressed in valence units = NH_4^+-O bond-valence parameters from Garcia-Rodriguez et al. (2000); all other bond-valence parameters from Brown and Altermatt (1985). The Al1-O and Al2-O bond strengths are based upon the refined Al/Fe site occupancies.

Utah. It seems remarkable that the new mineral carlsonite has not previously been reported from other NH_4 mineral occurrences and particularly from those in which these phases have formed by deposition from high-temperature gases. There are sufficient similarities in the powder X-ray diffraction patterns of carlsonite and metavoltine to suspect that carlsonite may have been mistaken for metavoltine in some previous studies of NH_4-rich mineral assemblages.

The new heteropolyhedral cluster in the structure of huizingite-(Al) is of interest simply because of its uniqueness, but more so because of insight that its existence may provide into the structural and paragenetic relations among the various hydrated ferric sulfate minerals. In particular, it may exist as a complex in aqueous solutions or in solid-state transformations involving the formation and/or breakdown of sideronatrite-style $[Fe^{3+}(SO_4)_3]^{3-}$ chains. The fact that it has thus far only been found in a rare phase formed under extreme and very ephemeral conditions suggests that it has a very narrow stability range and its existence is normally transitory.

Acknowledgments

Uwe Kolitsch and an anonymous reviewer provided constructive comments on the manuscript. Frank Hawthorne is thanked for suggestions regarding the discussion of Lewis acidity-basicity. Will Shewfelt is acknowledged for bringing this mineral occurrence to the attention of the scientific community via the late Ernest Carlson of Kent State University. Ernest Carlson and Lance Kearns of John Madison University and George Robinson of the A.E. Seaman Mineralogical Museum (Michigan Technological University) are acknowledged for initial studies on the minerals from this occurrence. We are grateful to Andy Sommer of Miami University for use of his Raman and FTIR instruments and help with FTIR data collection. The electron microprobe laboratory at the University of Utah is supported in part by the National Science Foundation, the College of Mines and Earth Sciences, and the Department of Geology and Geophysics. Wil Mace of that department is acknowledged for assistance with the microprobe analyses. The SEM/EDS laboratory at Oberlin College, which provided initial recognition of most of the phases at the burn site, is partly supported by the National Science Foundation. A portion of this investigation was funded by the John Jago Trelawney Endowment to the Mineral Sciences Department of the Natural History Museum of Los Angeles County.

References cited

Brese, N.E., and O'Keeffe, M. (1991) Bond-valence parameters for solids. Acta Crystallographica, B47, 192–197.

Brown, I.D. (1981) The bond-valence method: an empirical approach to chemical structure and bonding. In M. O'Keeffe and A. Navrotsky, Eds., Structure and Bonding in Crystals, 2, p. 1–30. Academic Press, New York.

Brown, I.D., and Altermatt, D. (1985) Bond-valence parameters from a systematic analysis of the inorganic crystal structure database. Acta Crystallographica, B41, 244–247.

Burla, M.C., Caliandro, R., Camalli, M., Carrozzini, B., Cascarano, G.L., De Caro, L., Giacovazzo, C., Polidori, G., and Spagna, R. (2005) SIR2004: an improved tool for crystal structure determination and refinement. Journal of Applied Crystallography, 38, 381–388.

Catti, M., and Franchini-Angela, M. (1976) Hydrogen bonding in the crystalline state. Structure of $Mg_3(NH_4)_2(HPO_4)_4 \cdot 8H_2O$ (hannayite), and crystal-chemical relationships with schertelite and struvite. Acta Crystallographica, B32, 2842–2848.

Demartin, F., Gramaccioli, C.M., and Campostrini, I. (2010) Pyracmonite, $(NH_4)_3Fe(SO_4)_3$, a new ammonium iron sulfate from La Fossa Crater, Vulcano, Aeolian Islands, Italy. Canadian Mineralogist, 48, 307–313.

García-Rodríguez, L., Rute-Pérez, Á., Piñero, J.R., and González-Silgo, C. (2000) Bond-valence parameters for ammonium-anion interactions. Acta Crystallographica, B56, 565–569.

Giacovazzo, C., Scordari, F., Todisco, A., and Menchetti, S. (1976) Crystal structure model for metavoltine from Sierra Gorda. Tschermaks Mineralogische und Petrographische Mitteilungen, 23, 155–166.

Hawthorne, F.C. (2012) A bond-topological approach to theoretical mineralogy: crystal structure, chemical composition and chemical reactions. Physics and Chemistry of Minerals, 39, 841–874.

Hawthorne, F.C., and Schindler, M. (2008) Understanding the weakly bonded constituents in oxysalt minerals. Zeitschrift für Kristallographie, 223, 41–68.

Higashi, T. (2001) ABSCOR. Rigaku Corporation, Tokyo.

Hoover, K.V. (1960) Devonian-Mississippian shale sequence in Ohio. Ohio Division of Geological Survey, Informational Circular 27, 154 p.

Kampf, A.R., Richards, R.P., and Nash, B.P. (2014) The 2*H* and 3*R* polytypes of sabieite, $NH_4Fe^{3+}(SO_4)_2$, from a natural fire in an oil-bearing shale near Milan, Ohio. American Mineralogist, 98, 1500–1506.

Khan, A.A., and Baur, W.H. (1972) Salt hydrates. VIII. The crystal structures of sodium ammonium orthochromate dihydrate and magnesium diammonium bis(hydrogen orthophosphate) tetrahydrate and a discussion of the ammonium ion. Acta Crystallographica, B28, 683–693.

Knop, O., Cameron, T.S., Deraniyagala, S.P., Adhikesavalu, D., and Falk, M. (1985) Infrared spectra of the ammonium ion in crystals. Part XIII. Crystal structure of $(NH_4)_2[AlF_5(H_2O)]$ and NH_3D^+ probe-ion spectra in $(NH_4)_2[AlF_5(H_2O)]$, NH_4AlF_4, and $(NH_4)_3ZnCl_5$, with remarks on structural filiation of AMF_4 fluorides. Canadian Journal of Chemistry, 63, 516–525.

Mandarino, J.A. (2007) The Gladstone-Dale compatibility of minerals and its use in selecting mineral species for further study. Canadian Mineralogist, 45, 1307–1324.

Martini, J.E.J. (1983) Lonecreekite, sabieite, and clairite, new secondary ammonium ferric-iron sulfates from Lone Creek Fall cave, near Sabie, eastern Transvaal. Annals of the Geological Survey of South Africa, 17, 29–34.

Mootz, V.-D., and Wunderlich, H. (1970) Die Kristallstruktur von $(NH_4)_3PO_4 \cdot 3H_2O$, Triammonium-orthophosphat-trihydrat. Acta Crystallographica, B26, 1826–1835 (in German).

Nakamoto, K. (1986) Infrared and Raman Spectra of Inorganic and Coordination Compounds. Wiley, New York.

Parafiniuk, J., and Kruszewski, L. (2009) Ammonium minerals from burning coal-dumps of the Upper Silesian Coal Basin (Poland). Geological Quarterly, 53, 341–356.

Pouchou, J.-L., and Pichoir, F. (1991) Quantitative analysis of homogeneous or stratified microvolumes applying the model "PAP". In K.F.J. Heinrich and D.E. Newbury, Eds., Electron Probe Quantitation, p. 3l–75. Plenum Press, New York.

Schindler, M., and Hawthorne, F.C. (2001) A bond-valence approach to the structure, chemistry, and paragenesis of hydroxyl-hydrated oxysalt minerals. I. Theory. Canadian Mineralogist, 39, 1225–1242.

Scordari, F., and Ventruti, G. (2009) Sideronatrite, $Na_2Fe(SO_4)_2(OH) \cdot 3H_2O$: Crystal structure of the orthorhombic polytype and OD character analysis. American Mineralogist, 94, 1679–1686.

Scordari, F., Stasi, F., Schingaro, E., and Comunale, G. (1994) A survey of $(Na,H_3O^+,K)_5Fe_3O(SO_4)_6 \cdot H_2O$ compounds: architectural principles and influence of the Na–K replacement on their structures. Crystal structure, solid-state transformation and its relationship to some analogues. Zeitschrift für Kristallographie, 209, 733–737.

Sheldrick, G.M. (2008) A short history of SHELX. Acta Crystallographica, A64, 112–122.

Szakall, S., Sajo, I., Feher, B., and Bigi, S. (2012) Ammoniomagnesiovoltaite, a new voltaite-related mineral species from Pécs-Vasas, Hungary. Canadian Mineralogist, 50, 65–72.

Wendlandt, R.F., and Harrison, W.J. (2006) Ammonium sulfate evaporites associated with uranium mill tailings disposal cells. American Geophysical Union, Fall Meeting 2006, abstract V31D-0603.

Witzke, T., de Wit, F., Kolitsch, U., and Blass, G. (2015) Mineralogy of the burning Anna I coal mine dump, Alsdorf, Germany. In G.B. Stracher, A. Prakash, and E.V. Sokol, Eds., Coal and Peat Fires: A Global Perspective, Case studies—coal fires, 3, chapter 7, p. 203–240. Elsevier.

Manuscript received January 12, 2016
Manuscript accepted April 21, 2016
Manuscript handled by G. Diego Gatta